University of Central Florida
STARS

Electronic Theses and Dissertations, 2020-

2022

Autoignition Delay Time Measurements and Chemical Kinetic Modeling of Hydrogen/Ammonia/Natural Gas Mixtures

Jessica Baker
University of Central Florida

 Part of the Aerodynamics and Fluid Mechanics Commons, and the Mechanical Engineering Commons
Find similar works at: https://stars.library.ucf.edu/etd2020
University of Central Florida Libraries http://library.ucf.edu

This Masters Thesis (Open Access) is brought to you for free and open access by STARS. It has been accepted for inclusion in Electronic Theses and Dissertations, 2020- by an authorized administrator of STARS. For more information, please contact STARS@ucf.edu.

STARS Citation
Baker, Jessica, "Autoignition Delay Time Measurements and Chemical Kinetic Modeling of Hydrogen/Ammonia/Natural Gas Mixtures" (2022). *Electronic Theses and Dissertations, 2020-*. 1361.
https://stars.library.ucf.edu/etd2020/1361

AUTOIGNITION DELAY TIME MEASURMENTS AND CHEMICAL KINETIC MODELING OF HYDROGEN/AMMONIA/NATURAL GAS MIXTURES

by

JESSICA BLUE BAKER
B.S. University of Central Florida, 2020

A thesis submitted in partial fulfillment of the requirements
for the degree of Master of Science
in the Department of Mechanical and Aerospace Engineering
in the College of Engineering and Computer Science
at the University of Central Florida
Orlando, Florida

Fall Term
2022

© 2022 Jessica Blue Baker

ABSTRACT

In recent years, hydrogen-carrying compounds have accrued interest as an alternative to traditional fossil fuels due to their function as zero-emission fuels. As such, there is interest in investigating hydrogen-carrying compounds to improve understanding of the fuels' characteristics for use in high pressure systems. In the current study, the oxidation of ammonia/natural gas/hydrogen mixtures was carried out to study CO formation profiles as well as the ignition delay times behind reflected shock waves in order to refine chemical kinetic models. Experiments were carried out in the University of Central Florida's shock tube facility by utilizing chemiluminescence to obtain OH* emission and laser absorption spectroscopy to obtain CO profiles over a temperature range between 1200 K to 1800 K with an average pressure of 2.2 atm. Experimental mixtures included both neat and combination natural gas/hydrogen with ammonia addition, with all mixtures except one having an equivalence ratio of 1. Results were then compared with the GRI 3.0 mechanism, as well as the newly developed UCF 2022 mechanism utilizing CHEMKIN-Pro software.

In general, both models were able to capture the trend in autoignition delay times and CO time histories for natural gas and ammonia mixtures. However, for ammonia-hydrogen mixtures, GRI 3.0 failed to predict ignition delay times, whereas the UCF 2022 mechanism was able to capture the IDTs within the uncertainty limits of the experiments. A sensitivity analysis was conducted for different mixtures to understand the important reactions at the experimental conditions. Finally, a reaction pathway analysis was carried out to understand important ammonia decomposition pathways in the presence of hydrogen and natural gas.

ACKNOWLEDGMENTS

I'd like to thank my advisor, Dr. Subith Vasu, for his support, assistance, and commitment to my growth throughout my studies. I would also like to thank my committee members Dr. Richard Blair and Dr. Anthony Terracciano for their time and willingness to be on this committee.

Thank you to my coworkers and friends at the lab and especially to Rosa Olivera and Dr. Ramees K. Rahman, whose help was invaluable. Thank you to my family and friends for their love and support.

The authors thank NASA (Grant Number 80NSSC21K2056), the Department of Energy (DE-FE0032072), the NASA Florida Space Grant Consortium, and UCF for supporting this work.

Disclaimer: This report was prepared as an account of work sponsored by an agency of the U.S. Government. Neither the U.S. Government nor any agency thereof, nor any of their employees, makes any warranty, express or implied, or assumes any legal liability or responsibility for the accuracy, completeness, or usefulness of any information, apparatus, product, or process disclosed or represents that its use would not infringe privately owned rights. Reference herein to any specific commercial product, process, or service by trade name, trademark, manufacturer, or otherwise does not necessarily constitute or imply its endorsement, recommendation, or favoring by the U.S. Government or any agency thereof. The views and opinions of authors expressed herein do not necessarily state or reflect those of the U.S. Government or any agency thereof.

TABLE OF CONTENTS

LIST OF FIGURES

LIST OF TABLES

CHAPTER 1: INTRODUCTION

The United States Energy Information Administration has projected that worldwide carbon emissions will increase 0.6% per year through 2050 [1]. In order to minimize greenhouse gases and other toxic gas emissions and promote sustainability and efficient energy production, there has been interest in utilizing hydrogen (H2) and hydrogen-carrying compounds as a replacement fuel. Through movements such as the Paris Climate Agreement as well as the executive order in the U.S. to reach net-zero emissions by 2050 (with the intent to restrict government agencies to use 100% clean electricity by 2030), the idea of carbon-neutral cycles has accrued interest from multiple governments around the world as well as private companies looking to minimize their carbon footprint and decrease costs. Accordingly, there have been new initiatives to utilize H2 and H2-carriers (e.g., ammonia, NH_3) for zero-emission power generation. Hydrogen functions as a zero-emission fuel and, as a result, is highly desirable for use in various power systems as, when burned with oxygen, water is the only product. One of the key impediments to the widespread use of hydrogen is the high cost. Industry users have little incentive to transition to hydrogen fuels over the already-existing infrastructure for propane and natural gas, due to the increased cost for transportation and storage. For example, for large-scale power generation such as gas turbines, it would be preferable to use existing technologies and infrastructure for burning hydrogen fuels with natural gas. NH_3 is a hydrogen-carrier that has thermal properties similar to that of propane and could thereby utilize the already existing storage and transport facilities. NH_3 has gained international interest as a fuel due to this already existing infrastructure and comparable energy density [2]. Such natural gas blends are essential to the future of clean energy.

CHAPTER 2: LITERATURE REVIEW

Ammonia's use as a fuel was previously studied in the 1960s, but early shock tube studies showed low accuracy and repeatability [3-9]. More recently, ammonia oxidation has accrued increased interest and has had its ignition characteristics studied under a wide set of temperatures and pressures. He et al. studied ammonia oxidation mixtures at 20 and 60 bar in a rapid compression machine while Song et al. investigated ammonia oxidation reactions at pressures of 30 and 100 bar in a laminar flow reactor; also, Iki et al. investigated the use of ammonia as a fuel in a micro gas turbine [10-13]. Additionally, a study by Mathieu et al. looked into ammonia oxidation reactions at pressures of 1.4,11, and 30 atm and high dilution percentages (98/99% dilution) [14].

Some studies focus on ammonia/air and ammonia/syngas mixtures with NOx formation carried out with techniques ranging from modeling studies, laminar burning velocity studies, and shock tube studies [15-17]. For example, Mathieu et al. measured ignition delay times using syngas mixtures doped with ppm levels of ammonia using a shock tube. This study found that ammonia had little effect on ignition delay times throughout their pressure range of 1.5, 12, and 30 atm [18]. Shu et al. also carried out a shock tube study focusing on ammonia/air mixtures at pressures of 20 and 40 bar, investigating autoignition characteristics at these relatively high pressures [19]. Furthermore, Rodolfo et al. computationally investigated chemical kinetic modeling of ammonia/hydrogen/air mixtures by studying autoignition and flame speed and NO formation and found that hydrogen addition to ammonia could improve its combustion behavior [20].

Ammonia/hydrogen mixtures have also been studied more in recent years. Chen et al., for example, investigated the ignition delay times of ammonia/hydrogen blends in a shock tube at temperatures from 1020-1945 K and pressures from 1.2 to 10 atm with hydrogen fractions of 0, 5,

30, and 70% while Valera-Medina et al. studied lean premixed combustion of ammonia/hydrogen in swirling gas turbines combustors, finding high instability in equivalent NH_3/H_2 blends [21, 22]. There have also been multiple numerical and simulation-based studies. One carried out by Pochet et al. found that hydrogen addition to ammonia in a rapid compression machine promoted ignition delay times to a significant degree in the low temperature range (1000-1100 K) [23]. Li et al. also carried out a numerical study focusing on hydrogen addition to ammonia flames, finding increased reactivity of ammonia combustion with hydrogen addition [24].

Very little literature exists focused on ammonia/natural gas mixtures, especially the ignition characteristics. Most recently, Oh et al. investigated the laminar flame speeds and CO production of natural gas/ammonia mixtures in a spark-ignition engine and found that emissions increased with increasing air-fuel ratio and drastic reduction of CO_2 emissions with the introduction of ammonia as a replacement fuel at temperatures of 300 and 600 K [25]. Additionally, Ishaq et al. investigated ammonia/natural gas blends in a wind-energy based system and saw increased combustion efficiency with ammonia addition while Ito and Onishi have investigated ammonia/natural gas co-firing in a gas turbine, though these studies focus primarily on emissions in the combustor with no model comparisons of ignition characteristics [26-28]. While in the past, ammonia has been studied with biodiesel/diesel fuels in engines (resulting in similar energy replacement as an engine fuel), there are few present studies at these baseline conditions [29]. With such limited available literature, there is a strong need for experimental ignition delay times (IDTs) in order to properly understand the behavior of ammonia/natural gas combustion.

There is currently a gap in the literature for natural gas/ammonia ignition studies as well as natural gas/hydrogen studies with equivalent ammonia/hydrogen fractions. The current study

offers to improve the understanding of ignition and combustion behavior of hydrogen-carrier fuels with natural gas. The ignition delay times and carbon monoxide (CO) concentration time histories are reported using a shock tube and laser absorption spectroscopy. To the best of the authors' knowledge, this study provides novel shock tube measurements of NH_3/natural gas and H_2/natural gas mixtures at these relevant conditions, essential points to act as validation targets for further development of hydrogen and natural gas mechanisms. While this study focuses on natural gas + NH_3 and natural gas + H_2, mixtures of H_2/NH_3, neat H_2, and neat natural gas were also studied to provide a comparison at similar conditions.

CHAPTER 3: METHODOLOGY

3.1 Shock Tube Facility

Experiments for the combustion of NH_3/H_2 and natural gas/ NH_3 were carried out in the University of Central Florida's (UCF) facility containing a high-purity, stainless-steel shock tube having an inner diameter of 14.17 cm. Specific details of the facility can be found in earlier publications [30-32]. The velocity of the incident shock wave was measured using five piezoelectric pressure transducers (PCB 113B26; 500 kHz frequency response) equally spaced along the last 1.4 m of the shock tube linked to four time-interval counters (Agilent53220A; 0.1 ns time resolution). These incident shock velocity values were then linearly extrapolated to obtain the reflected shock velocity at the end wall location. The pressure and temperature after the reflected shock wave were calculated based on the extrapolated velocity, initial pressure, initial temperature, and normal 1-D shock relations. The test section consists of eight equally-spaced optical ports located 2 cm from the end wall, with one port being equipped with a pressure transducer (Kistler 603B1-piezoelectric). All measurements for this experimental campaign were taken at this 2 cm location.

Anhydrous ammonia and a research-grade ammonia/nitrogen mixture (>98% pure; Air Liquide), natural gas mixture (>99.99% purity; nexAir), oxygen (O_2; >99.99% purity; nexAir), and balance gases (nitrogen (N_2), argon (Ar); >99.99% purity; nexAir) were used to prepare the test mixtures, where the natural gas mixture is made up of 93% CH_4, 4.75% C_2H_6, 1.5% C_3H_8, and 0.75% C_4H_{10}. The mixtures were prepared manometrically in the 33 L Teflon coated, stainless steel mixing tank fitted with a magnetically driven stirrer to ensure homogeneity of the mixture, measuring the partial pressures with 100-Torr (MKS Instruments/Baratron E27D) and 10,000 Torr (MKS Instruments/Baratron 628D) full-scale range capacitance manometers during mixture

preparation and the filling process. Helium was used as the driver gas for all experiments. Test mixtures were allowed to homogenize for 4+ hours before experiments were carried out. The components of the test mixtures in this campaign can be seen in Table 1, all having an equivalence ratio of 1 except for mixture 4 which has an equivalence ratio of 0.767. Mixtures will henceforth be referred to by mixture number or M#.

Table 1: Components of Test Mixtures by Percentage

	Natural Gas	H_2	NH_3	O_2	N_2	Ar
Mixture 1	2	0	0	4.3	19	74.7
Mixture 2	1	1	0	2.65	19	76.35
Mixture 3	1	0	1	2.9	19	76.1
Mixture 4	1	0	0.1	2.9	19	77
Mixture 5	0	1	1	1.25	19	77.75
Mixture 6	0	2	0	1	19	78

Since ammonia has been known to adsorb on contact with stainless steel, all mixtures containing ammonia were prepared using a passivation technique during mixture preparation on the internal surface of the mixing tank as well as before each experiment on the internal surface of the shock tube, as suggested by Mathieu and Peterson [14]. During passivation of the mixing tank, ammonia was introduced to the system at an equivalent pressure to the desired partial pressure of ammonia in the mixture. The ammonia was allowed to adsorb for approximately 15 minutes before the tank was vacuumed down to <1 torr and the final mixtures could be prepared. Passivation of the shock tube took place before each experiment in a similar process. Ammonia was introduced to the shock tube at a pressure equal to the desired P1, allowed to adsorb for approximately 10 minutes, and was then vacuumed out to a pressure of 5E-5 torr before re-filling to the final P1.

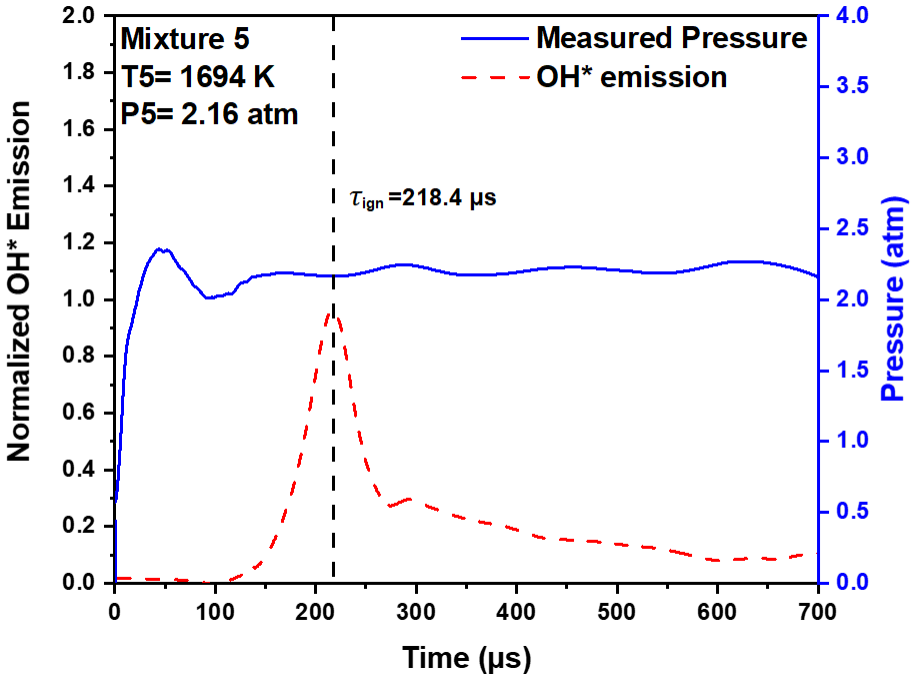

Figure 1: Pressure and Normalized OH* Emission Trace during Stoichiometric Ignition of Mixture 5 at 1694 K and 2.16 atm (OH* Emission Signal was Normalized to its Peak Value)

3.2 Experimental Measurements

Ignition delay times can be determined in multiple different ways and, depending on the definition, can result in differences of over 100 µs [33]. The definition selected for use for the current study is the time between the arrival of the reflected shockwave (determined from the pressure spike) to the time coinciding with the peak of the normalized emission signal at the sidewall location. A representative pressure and emission profile can be seen in Figure 1. Ignition delay time measurements were carried out via a photomultiplier tube (Model 2032) with a 310 ± 2 nm bandpass filter to isolate the OH* emission also at the 2 cm location from the end wall. The overall uncertainty in shock tube ignition delay time measurements is less than ±10%, resulting largely from uncertainty in mixture composition, thermodynamic parameters, and reflected shock temperatures. The uncertainty for the CO mole fraction is estimated via a time-varying root mean square quantity where the uncertainties from the parameters of Beer's Law (Equation 1) are taken

into account (these parameters include absorbance, pressure, temperature, and absorption cross-section). More information about this method can be found in Ninnemann et al. [34].

Carbon monoxide time histories were also measured for mixtures 1-4. These time histories measurements were also taken at the 2 cm location utilizing fixed wavelength absorption spectroscopy with a distributed feedback quantum cascade laser (DFB QCL) targeting a CO absorbance peak at 2046.28 cm^{-1}. A Bristol Spectrum Analyzer was used to periodically monitor the spectral output and ensure stability. A schematic for the shock tube and laser setup can be seen in Figure 2. The experimental mole fractions were obtained via the Beer-Lambert Law and absorbance equation given in Equations (1) and (2), respectively.

$$X_{CO} = \frac{(\alpha_v RT)}{\sigma \mathrm{PL}} \tag{1}$$

$$\alpha_v = -\ln\left(\frac{I}{I_o}\right)_v \tag{2}$$

Where α_v is the absorbance at frequency ν; R (J/mol-K) is the universal gas constant; T (K) is the temperature of the gas; σ (m^2/molecule) is the absorption cross-section of the absorbing species; P (Pa) is the pressure of the gas; L (m) is the path length of the shock tube; and in Equation (2), I and Io are the measured intensities of laser power in test gas mixture and in vacuum, respectively, at frequency ν. The absorption cross section values were obtained from HITRAN 2016 database at each P5 and T5 condition where absorbance from potential interfering species was negligible [35].

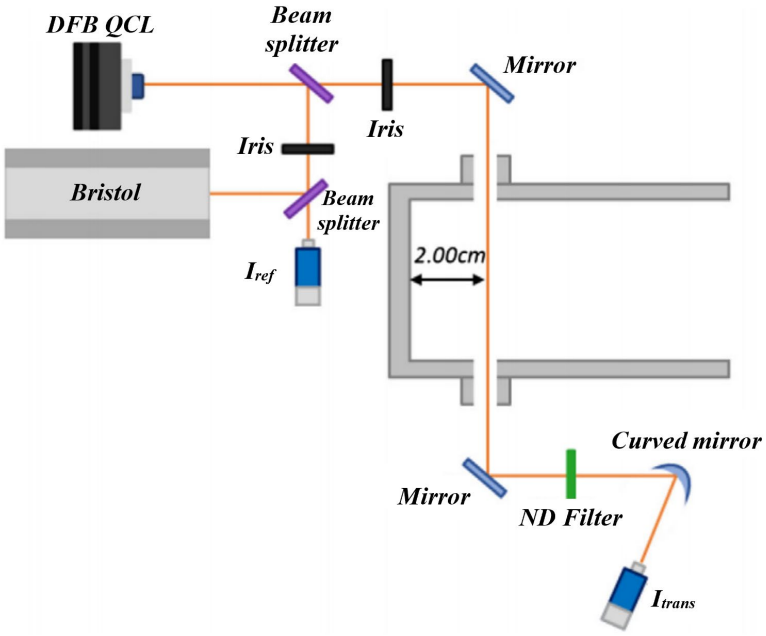

Figure 2: Schematic for the Shock Tube and Laser Diagnostic Setup

3.3 Chemical Kinetic Modeling

Numerical simulations of shock tube experiments were performed using CHEMKIN-Pro [36] with a closed (0-D) homogeneous batch reactor under adiabatic conditions with constant UV assumption. When the shock wave passes through the reaction mixture, the step change in temperature and pressure justifies the former assumption while the adiabatic assumption can be justified as the whole process takes place in less than 5 ms.

To simulate autoignition delay times and CO time histories for natural gas/hydrogen/ammonia mixtures, a kinetic model was developed using the base mechanism from Rahman et al. [37]. The Rahman et al. model is well validated for ignition delay times of methane oxidation for pressures up to 300 bar. It is also validated with experimental data for oxidation of smaller hydrocarbons in the presence of nitrogen oxides. However, this mechanism lacked reactions of C3 and C4 hydrocarbons which were added from the Aramco 3.0 mechanism [38]. Since this work focuses on oxidation studies with a nitrogen bath gas, the rates for the reactions

$N_2H_2 = NNH + H$ and $N_2H_2 + H = NNH + H_2$ were replaced with the rates from Dean and Bozzelli that are relevant to a nitrogen bath gas [39]. The new reaction mechanism consists of 121 species and 1040 reactions and will be referred to as the 'UCF 2022' mechanism hereafter. The reaction mechanism is available from authors upon request. Model results reported here include simulations using the UCF 2022 and GRI 3.0 mechanisms. The hydrocarbon C_4H_{10} from the natural gas mixture was added to the next highest species component (C_3H_8) for the GRI 3.0 mechanism as it does not contain this higher hydrocarbon.

CHAPTER 4: RESULTS

4.1 Experimental Measurements

4.1.1 Comparison of Experimental Ignition Delay Times during Natural Gas Oxidation and Effect of Hydrogen-Carriers Addition to Neat Natural Gas

Shock tube ignition delay times of neat natural gas are offered as a comparison to observe the effect that hydrogen-carrying compounds have on the baseline neat mixture. The experimental data with best fit lines can be seen in Figure 3 with neat natural gas shown as the baseline. It is apparent that hydrogen addition to natural gas promotes ignition on a large scale, while ammonia addition slows down the ignition. For 1% natural gas + 1% ammonia, the ignition delay time decreases by almost a factor of two while for 1% natural gas, 0.1% ammonia, the ignition delay time increases, more so at higher temperatures than compared with the low temperature conditions. The latter can be attributed to the leaner equivalence ratio of mixture 4.

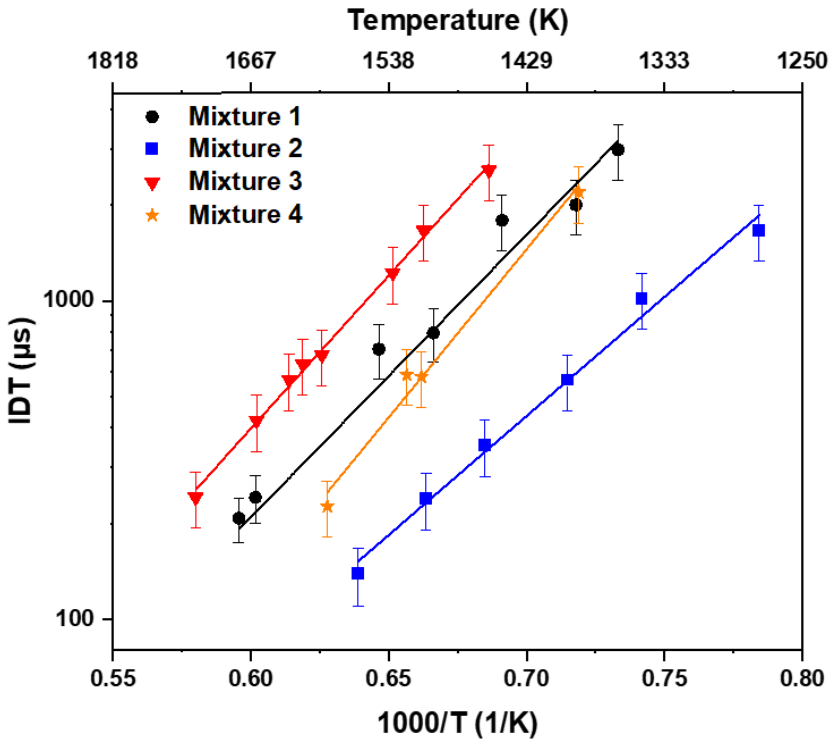

Figure 3: Comparison of Shock Tube Ignition Delay Times during Natural Gas Oxidation and Effect of Hydrogen-Carrier Compound Addition via H_2 and NH_3 to Natural Gas with Best Fit Lines

4.1.2 Comparison of Experimental Ignition Delay Times during Hydrogen Oxidation and Effect of Hydrogen-Carriers Addition to Neat Natural Gas

Shock tube ignition delay times of neat hydrogen are offered as a comparison to observe the effect of the addition of hydrogen-carrying compounds to the baseline neat mixture. The experimental data with best fit lines can be seen in Figure 4 with neat hydrogen as the baseline. It can be seen that with the addition of a hydrogen-carrying compound, the ignition delay time of the mixture increases as compared to the neat hydrogen case. For mixture 5, the slope mirrors that of the neat H_2 case while mixture 2 varies in slope. Both mixtures 2 and 5 show a strong increase in the trend of ignition delay times, with the ignition delay time of the mixtures doubling that of the neat H_2 case.

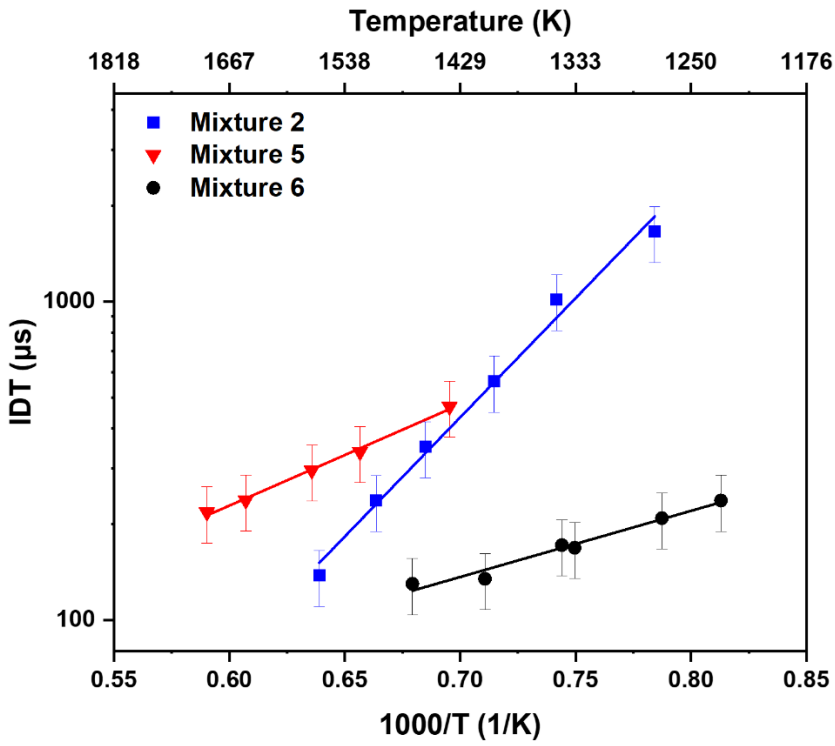

Figure 4: Comparison of Shock Tube Ignition Delay Times During Hydrogen Oxidation and Effect of Hydrogen-Carrier Compound Addition via Natural Gas and NH_3 to Hydrogen with Best Fit Lines

4.1.3 Comparison of Experimental Ignition Delay Times during Hydrogen Oxidation and Effect of Hydrogen-Carriers Addition to Neat Natural Gas

Figure 5 shows a comparison between CO production during combustion of natural gas + hydrogen-carrier compound at low and high temperature conditions. In general, each mixture shows the expected trend of the elevated temperature condition resulting in faster CO formation. The elevated temperature and pressure due to the combustion process causes natural gas to oxidize rapidly, leading to the steep increase in CO mole fraction seen in the high temperature conditions.

When comparing H_2 addition to the neat natural gas case, it is found that at the low temperature conditions, mixture 2 (Figure 6) shows increased CO production when compared to the baseline mixture 1 (Figure 5) at much lower temperature. This is because the hydrogen added to mixture 2 enhances the reaction progress. Mixture 3 (Figure 7), which contains 1% ammonia

needs a higher temperature (~1509 K) for CO to form in significant amounts compared to the baseline mixture 1. At similar temperatures (~1390 K), mixture 4 produces less CO (Figure 8) compared to mixture 1 at the end of test time. This is due to the combined effect of lower natural gas concentration (1% natural gas) and ammonia addition slowing the reaction progress. For the high temperature condition, mixtures 2, 3, and 4 (Figures 6, 7, 8) show a large drop in CO production as compared to mixture 1 (Figure 5). This is attributed to the higher concentration of natural gas in mixture 1 (2%) compared to other mixtures. For the high temperature condition, the peak concentration of mixture 4 (which has 0.1% NH_3 addition) is now much closer in scale to the CO production of mixtures 2 and 3 than at the low temperature condition, indicating dependence on temperature.

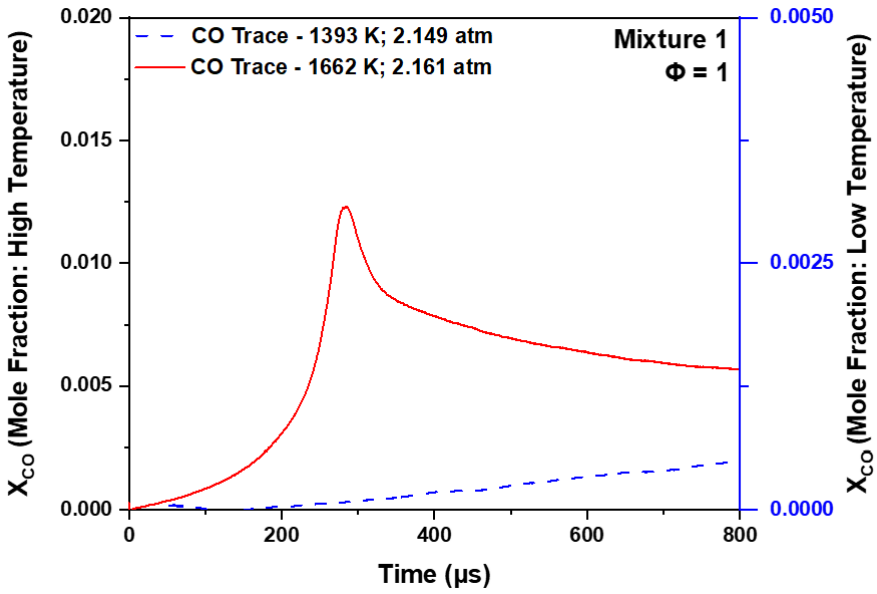

Figure 5: CO Formation during Combustion of Neat Mixtures 1 at Low Temperature Condition and High Temperature Condition

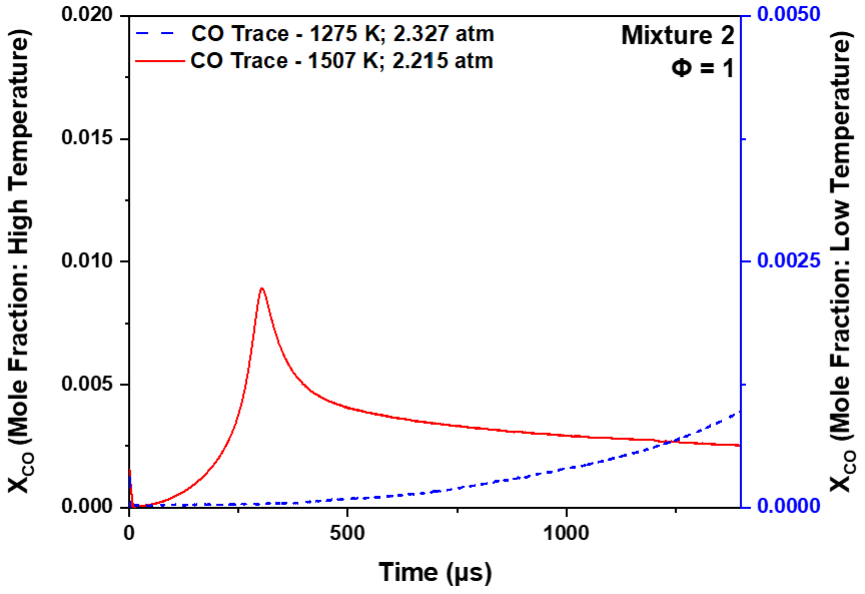

Figure 6: CO Formation During Combustion of Mixture 2 at Low Temperature Condition and High Temperature Condition

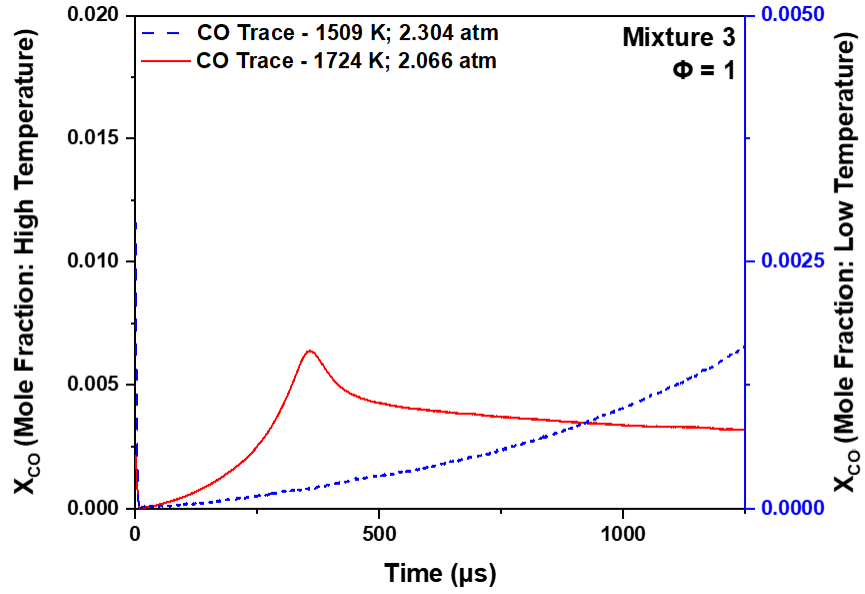

Figure 7: CO Formation during Combustion of Mixture 3 at Low Temperature Condition and High Temperature Condition

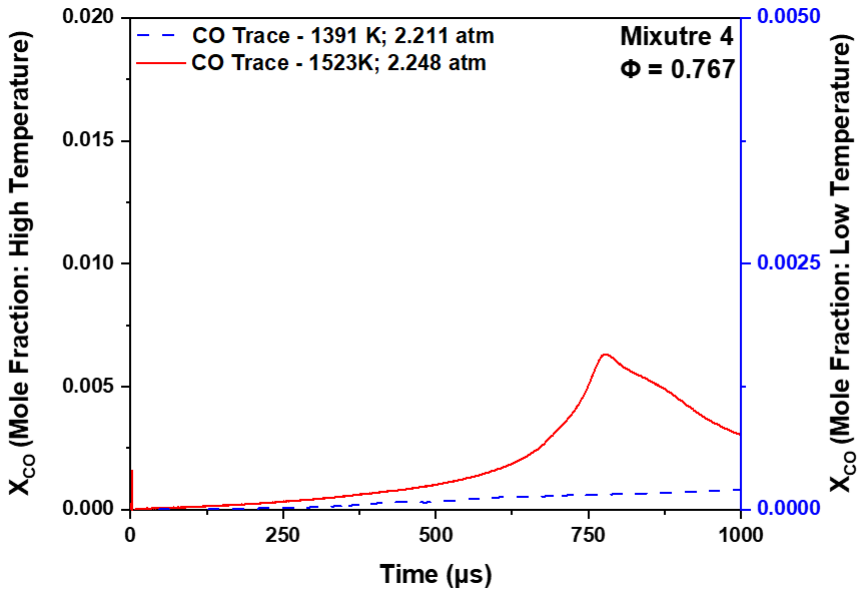

Figure 8: CO Formation during Combustion of Mixture 4 at Low Temperature Condition and High Temperature Condition

It can be noted that the low and high temperatures between mixtures are varying. This is due to the fact that some mixtures have faster ignition and form CO at lower temperatures while others were slow to ignite. The low temperature condition for each mixture was selected as the temperature close to where detectable amounts of CO was formed within the test time available during experiments (~0.8-1.5ms). The high temperature condition for each mixture was chosen so that the important features of the CO time history (steep increase, peak, consumption) were clearly visible. The difference in temperature between the mixtures is primarily due to the combustion properties of individual components in each mixture. For example, mixture 2 (1 % natural gas + 1% hydrogen) requires only 1275 K to produce CO within test times (Figure 6), due to the presence of hydrogen. However, mixture 3 (1% natural gas + 1% ammonia) does not produce detectable amounts of CO at this temperature and requires higher temperatures (~1500 K, Figure 7) to form CO within the test time.

4.2 Model Validation

4.2.1 Cases without NH3: Model Comparisons Using UCF 2022 and GRI 3.0 Mechanism

Figures 9-11 shows the model comparison with neat mixture 1, mixture 2, and neat mixture 6, as a baseline validation for the UCF 2022 model. The in-house model is compared with the industry standard GRI 3.0 mechanism in order to further confirm model functionality. It can be seen that both the UCF 2022 and GRI 3.0 models closely align with the experimental data, indicating a good baseline.

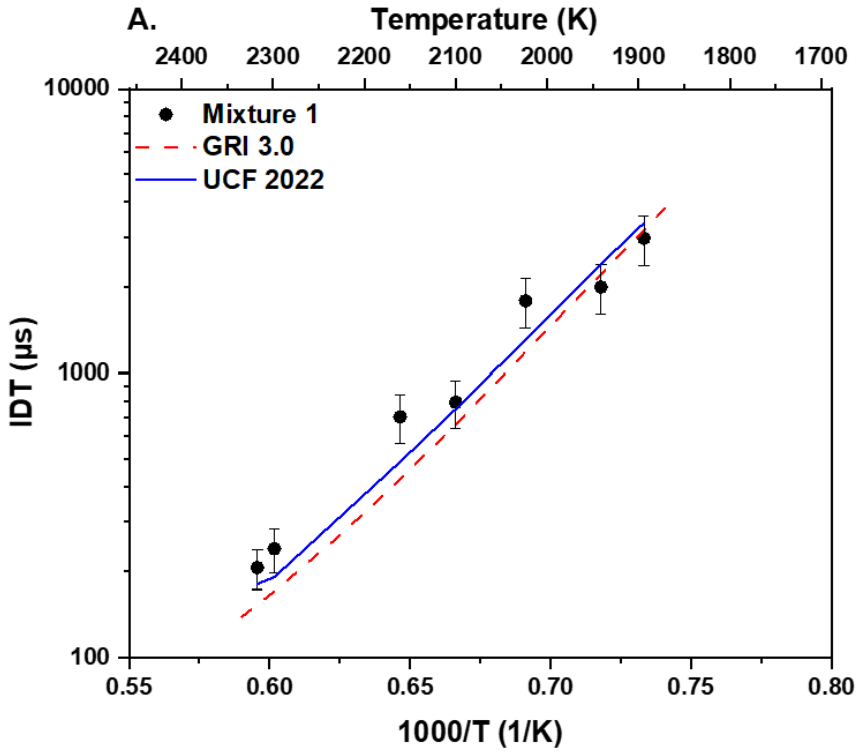

Figure 9: Comparison of Shock Tube Ignition Delay Times during Neat Mixture 1 Oxidation

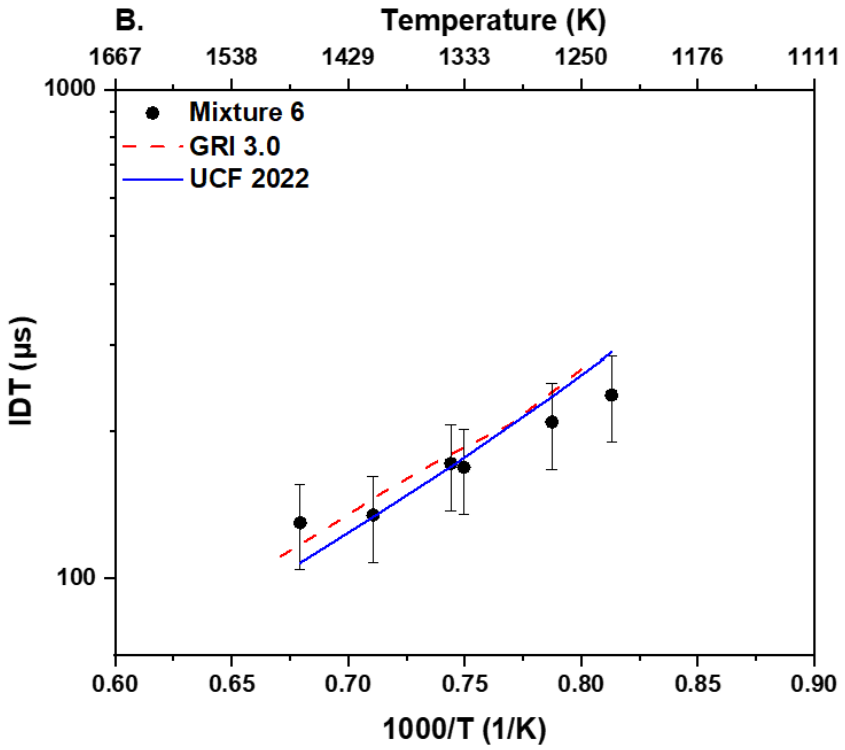

Figure 10: Comparison of Shock Tube Ignition Delay Times during Neat Mixture 6 Oxidation

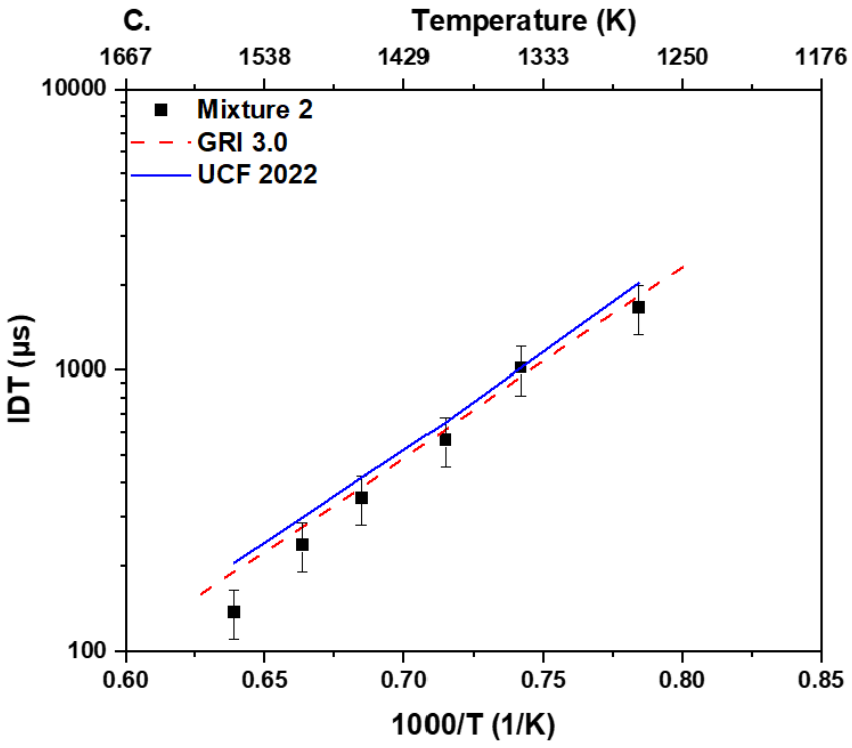

Figure 11: Comparison of Shock Tube Ignition Delay Times during Mixture 2 Oxidation

4.2.2 Cases with NH3: Model Comparisons Using UCF 2022 and GRI 3.0 Mechanism

Figures 12-14 shows the model comparison for all mixtures containing ammonia as the additive for the hydrogen-carrying compound as a baseline before adjustments were made to the model. The UCF 2022 mechanism is shown along with the GRI 3.0 mechanism in order to compare model functionality. It can be seen that neither model is fully able to accurately capture the combustion chemistry of ammonia when added to baseline H_2 or natural gas. For mixture 3, as well as mixture 4, both the GRI 3.0 mechanism and the UCF 2022 mechanism are within the margin of error. For mixture 3, there is more variation from the model at low temperatures, where the UCF 2022 model trends closer to the experimental data. However, for the mixture 5 case, the GRI 3.0 model greatly overpredicts the IDTs while the UCF 2022 model aligns well at lower temperatures and is still within the margin of error for the experimental points at higher temperatures.

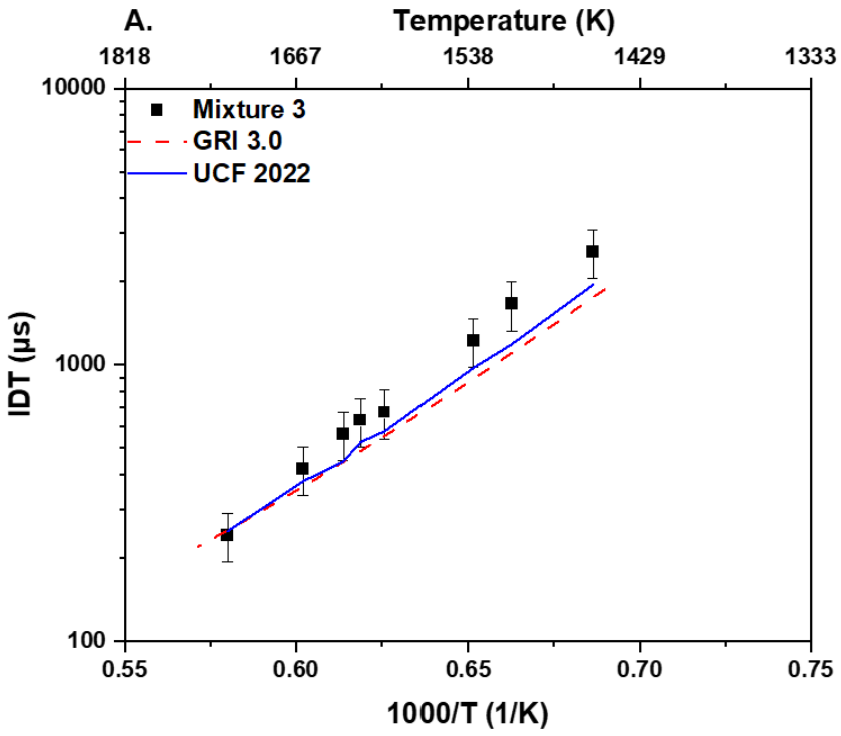

Figure 12: Comparison of Shock Tube Ignition Delay Times During Mixture 3 Oxidation

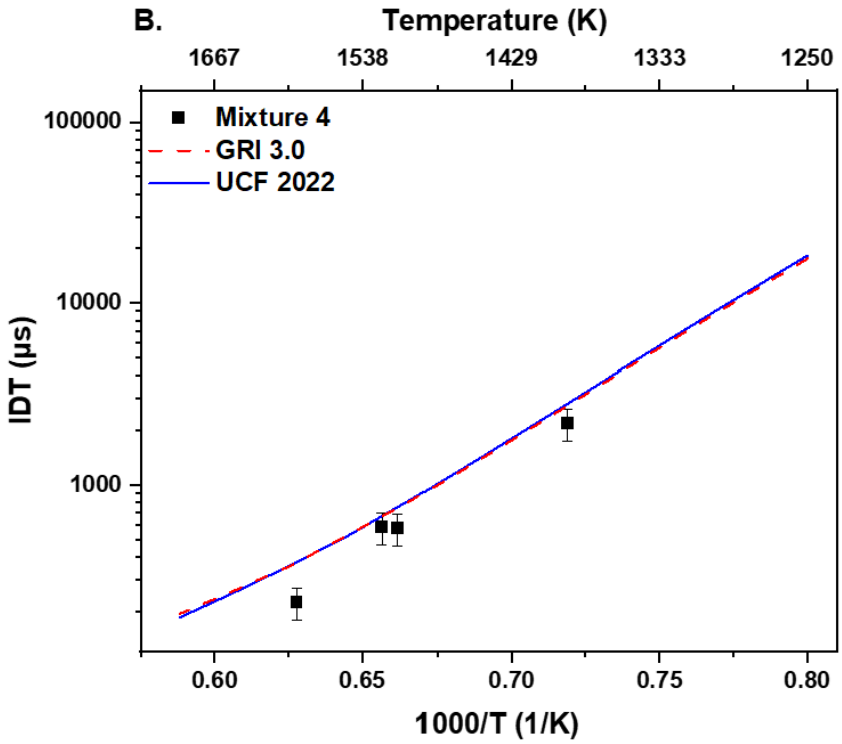

Figure 13: Comparison of Shock Tube Ignition Delay Times During Mixture 4 Oxidation

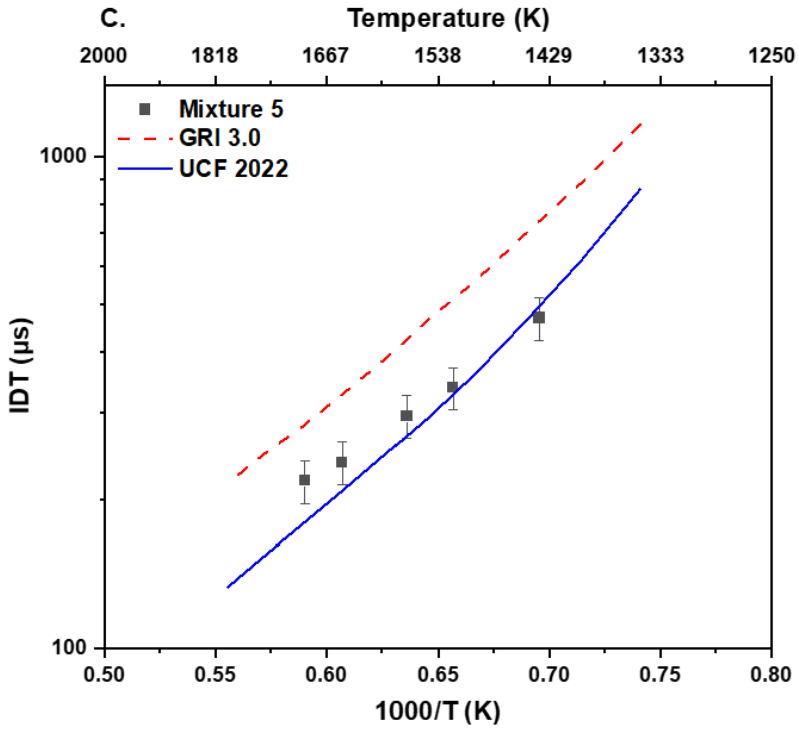

Figure 14: Comparison of Shock Tube Ignition Delay Times During Mixture 5 Oxidation

4.2.3 Model Comparison with CO Time Histories

The experimental data obtained for CO time histories was used to validate the UCF 2022 model. The results are shown in Figures 15-17. For the neat mixture 1 case, both models underpredict CO formation at 1393 K. However, for mixtures 2 and 3, both models were able to capture CO time histories with reasonable accuracy with GRI 3.0 being closer to experimental results.

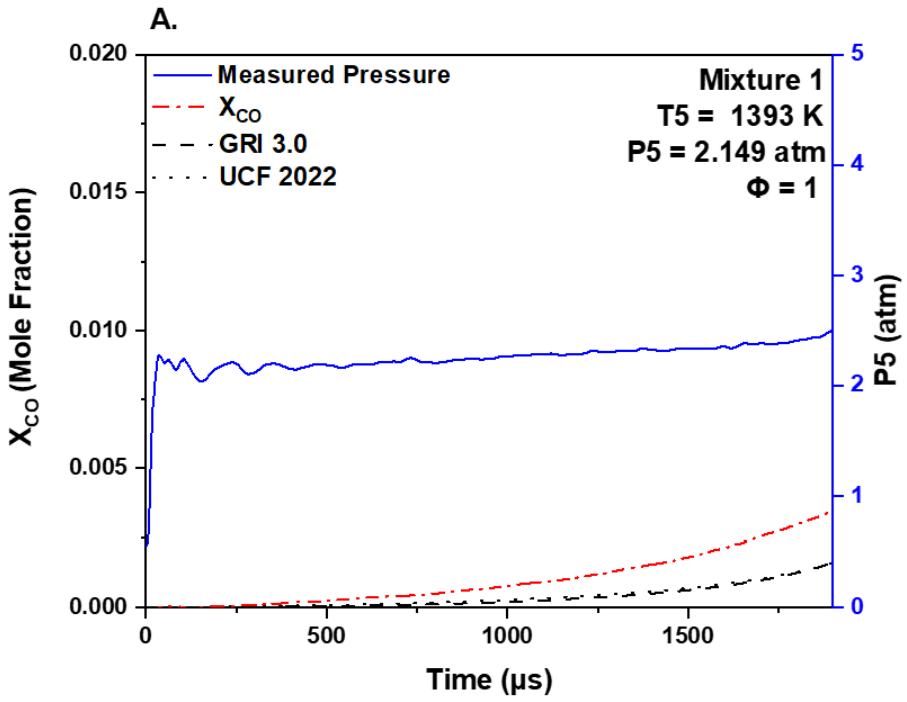

Figure 15: Comparison of CO Time Histories Predicted by GRI 3.0 and UCF 2022 Models with Experimental Results of Neat Mixture 1

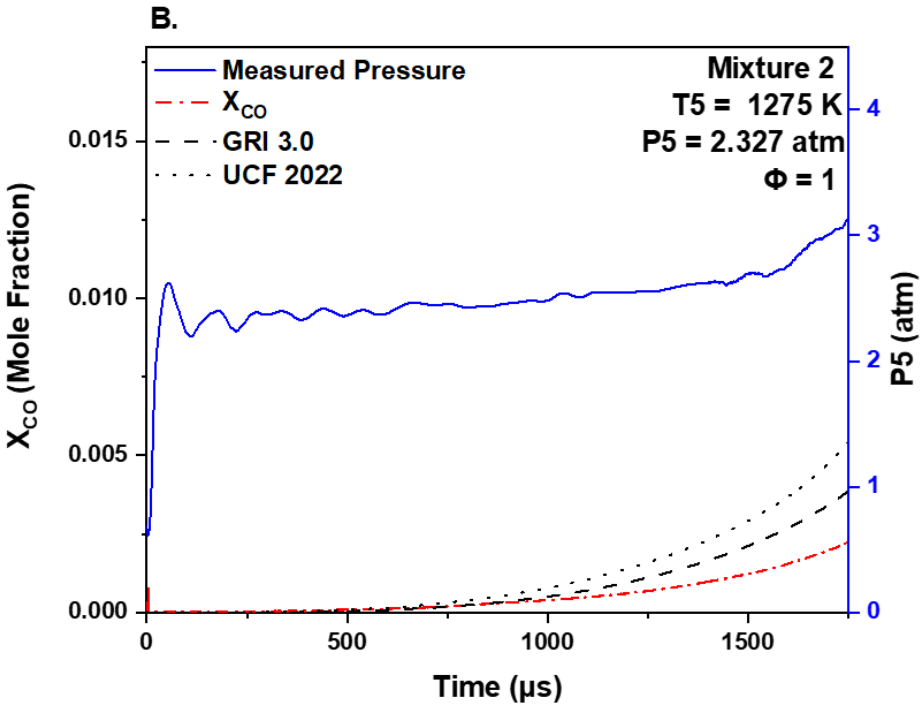

Figure 16: Comparison of CO Time Histories Predicted by GRI 3.0 and UCF 2022 Models with Experimental Results of Mixture 2

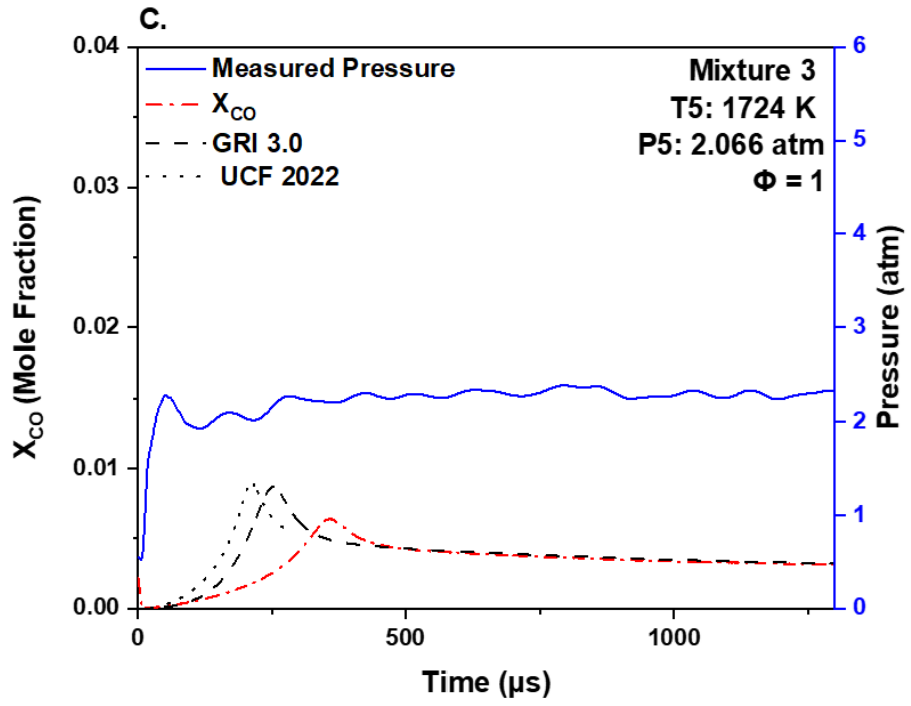

Figure 17: Comparison of CO Time Histories Predicted by GRI 3.0 and UCF 2022 Models with Experimental Results of Mixture 3

4.3 Sensitivity Analysis

4.3.1 Sensitivity Analysis at Various Conditions Comparing Experimental Data Using UCF 2022 Mechanism

The mechanism selected for use during the sensitivity analysis is the UCF 2022 mechanism. This was selected because, while both mechanisms match at certain conditions, the UCF mechanism is closer to the experimental data more often. OH* sensitivity analyses were carried out in order to identify key reactions that affect the ignition delay times of ammonia/natural gas and ammonia/hydrogen mixtures. IDT sensitivity analyses were done for critical reactions, and the specific reactions of interest were isolated, results of which can be seen in Figures 18-21.

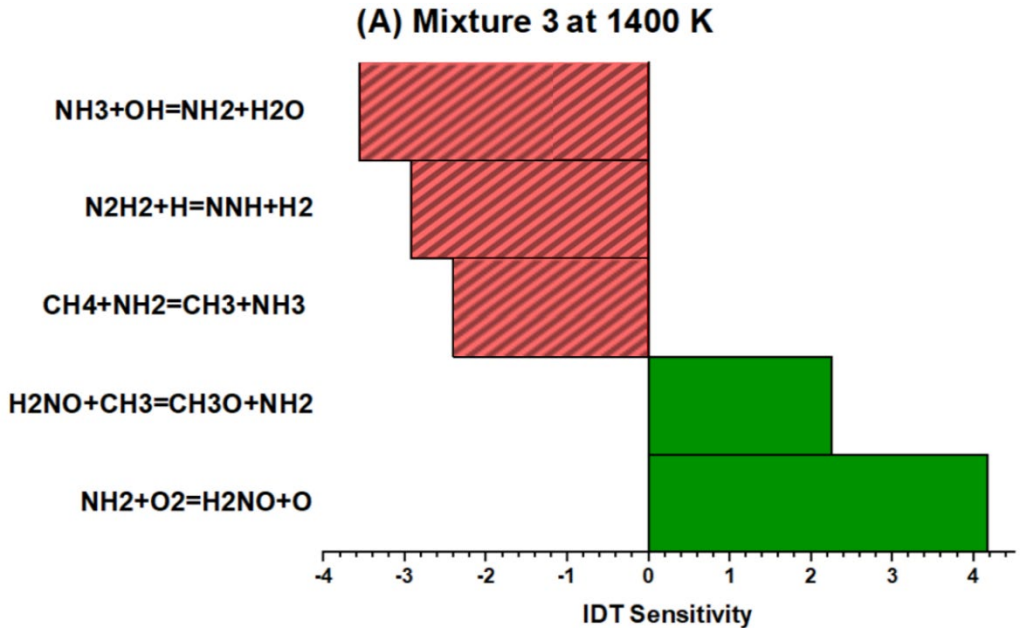

Figure 18: IDT Sensitivity Analysis for Mixture 3 at Low Temperature Condition. Conditions were Run at Average Pressure Of 2.2 atm; Red Bars: Negative Sensitivity, Green Bars: Positive Sensitivity

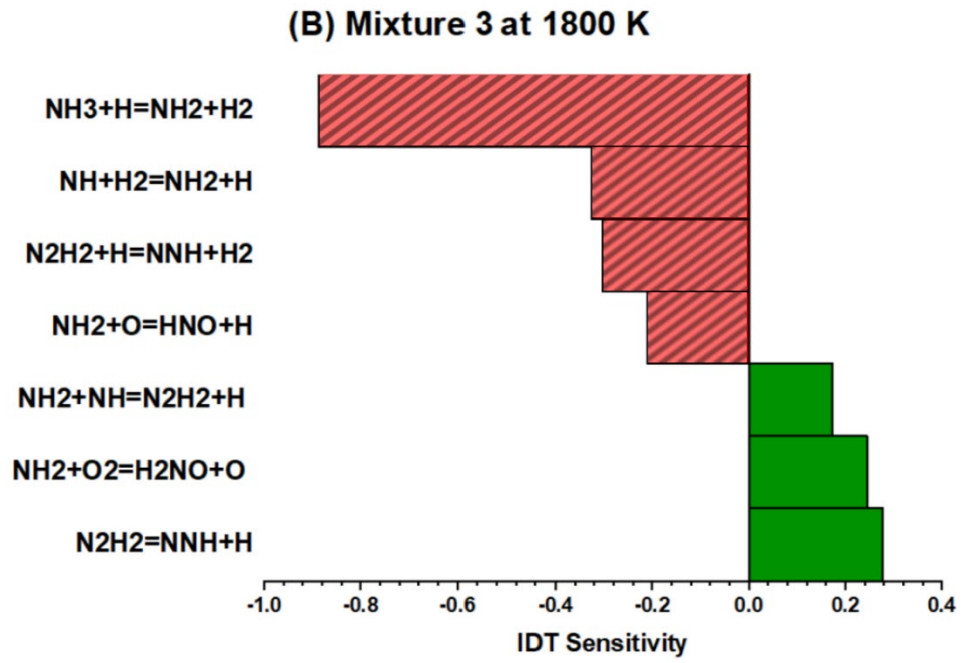

Figure 19: IDT Sensitivity Analysis for Mixture 3 at High Temperature Condition. Conditions were Run at Average Pressure Of 2.2 atm; Red Bars: Negative Sensitivity, Green Bars: Positive Sensitivity

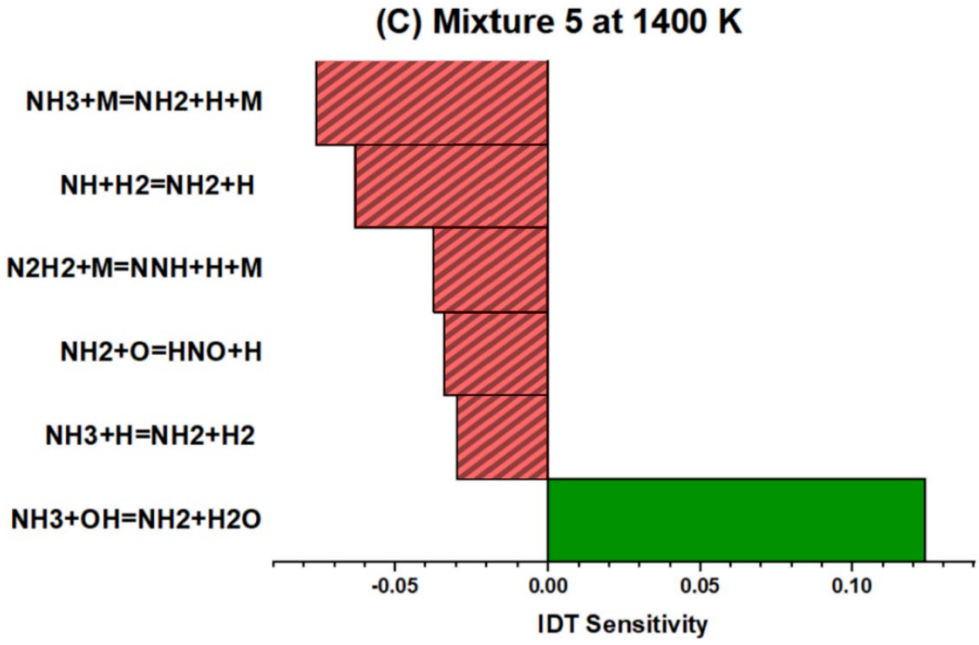

Figure 20: IDT Sensitivity Analysis for Mixture 5 at Low Temperature Condition. Conditions were Run at Average Pressure Of 2.2 atm; Red Bars: Negative Sensitivity, Green Bars: Positive Sensitivity

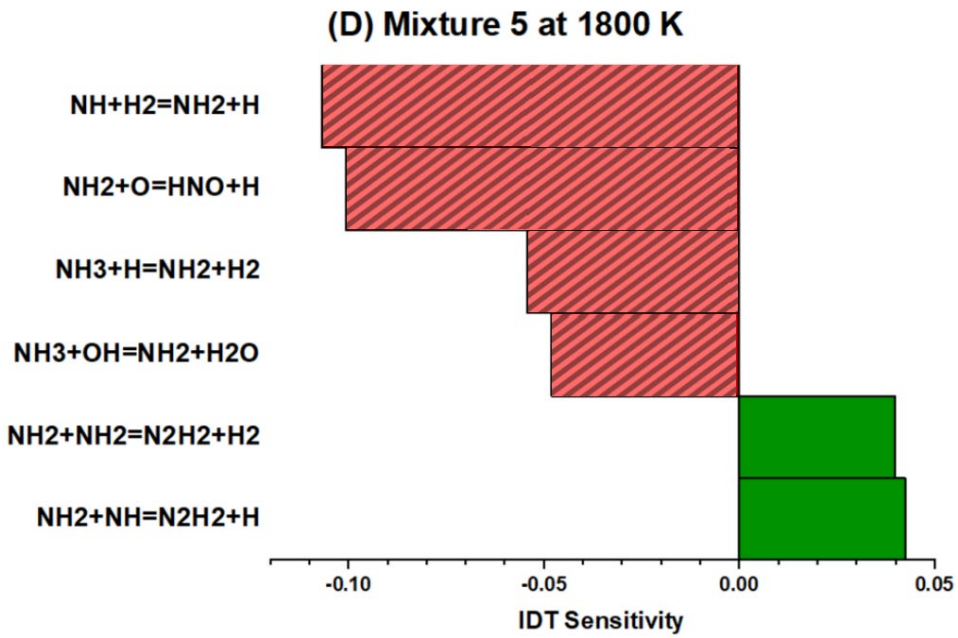

Figure 21: IDT Sensitivity Analysis for Mixture 5 at High Temperature Condition. Conditions were Run at Average Pressure Of 2.2 atm; Red Bars: Negative Sensitivity, Green Bars: Positive Sensitivity

A positive sensitivity indicates increased ignition delay times (lower reactivity) while a negative sensitivity value indicates lower ignition delay times and higher reactivity. The specific reactions of interest for this study include reactions due to the interaction of the hydrogen-carrier and the ammonia compound. As such, these specific reactions are the only ones shown in the sensitivity studies.

Between the two conditions for mixture 3 (both low and high temperatures), only two reactions, though they vary in sensitivity coefficient, are shared indicating a high dependence of the combustion chemistry on temperature. However, for the two mixture 5 studies (once again, low and high temperature), four reactions are shared between the two cases with the similar reactions being of closer scale than in the mixture 3 studies.

4.4 Reaction Pathway Analysis for Ammonia Oxidation with and without Carbonaceous Compounds

The reaction path analysis was carried out for high temperature oxidation of ammonia in the presence of hydrogen and natural gas to understand important reaction pathways involved in NO formation and ammonia decomposition. The UCF 2022 reaction mechanism was used for reaction path analysis as it predicted IDTs with a good degree of accuracy.

4.4.1 High Temperature NH3 Oxidation with Hydrogen (T=1600 K, P=2 atm)

The initiation of ammonia combustion in an ammonia oxidation mixture starts with the unimolecular decomposition of ammonia at high temperatures, resulting in the formation of NH_2 and the H radical. This reaction is highly dependent on temperature and is slow compared to hydrogen oxidation. However, hydrogen at 1600 K forms OH, H, and O radicals in the presence of oxygen. The high concentration of these radicals in the ammonia + hydrogen oxidation mixtures at high temperatures speeds up the decomposition of ammonia by H-abstraction reactions R1-R3.

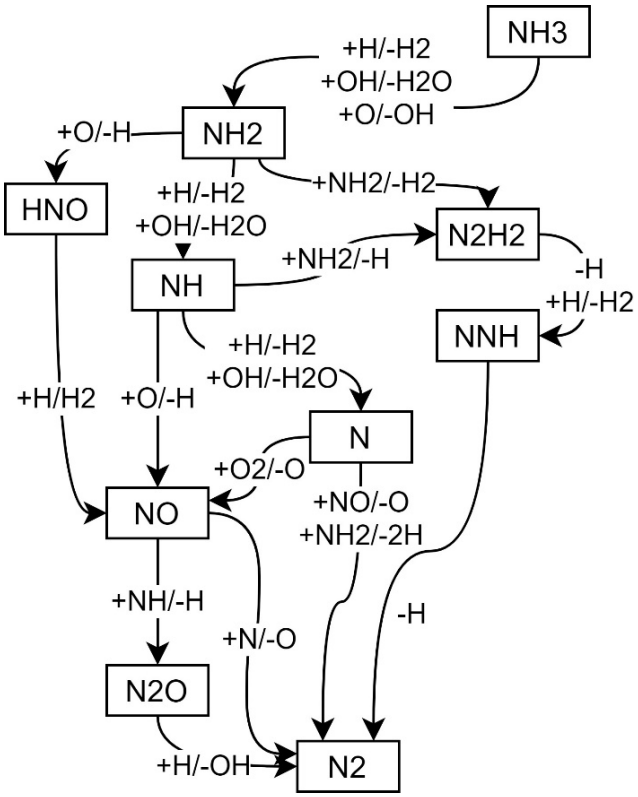

Figure 22: Reaction Pathway Diagram for High Temperature Oxidation of Ammonia in Ammonia + Hydrogen Oxidation Mixture at 1600 K and 2 atm

$NH_3 + OH = NH_2 + H_2O$ R1

$NH_3 + H = NH_2 + H_2$ R2

$NH_3 + O = NH_2 + OH$ R3

The NH_2 formed reacts with another NH_2 molecule to form N_2H_2 by reaction R4, which is one step where ammonia releases its hydrogen content. Ammonia also reacts with the H radical to release hydrogen and the NH_2 radical as shown in reaction R5. N_2H_2 reacts with H atoms to form NNH and releases hydrogen again. The NNH then decomposes into nitrogen and H atom.

$2NH_2 = N_2H_2 + H_2$ R4

$NH_3 + H = NH_2 + H_2$ R5

$N_2H_2 + H = NNH + H_2$ R6

NH_2 also reacts with O atoms to form HNO and releases H atoms (R7). The HNO formed then reacts with the H radical and releases NO. This is one of the primary pathways to the formation of NO from ammonia. Another pathway for NO formation is from NH which is formed by H-abstraction of NH_2 by H and OH radicals as shown in reactions R8 and R9.

$NH_2 + O = HNO + H$ R7

$NH_2 + H = NH + H_2$ R8

$NH_2 + OH = NH + H_2O$ R9

NH also reacts with NO to form N_2O and then undergoes H-abstraction to form nitrogen atoms, both of which eventually form a stable nitrogen molecule as shown in Figure 22.

4.4.2 High Temperature NH3 Oxidation with Natural Gas (T=1600 K, P=2 atm)

Figure 23 shows the reaction pathway diagram for ammonia oxidation in the presence of natural gas. Similar to the case with hydrogen in the ammonia + hydrogen mixture, a significant amount of H, OH, and O radicals are created by the initial reactions of larger hydrocarbons (C_3H_8, C_4H_{10}, etc.) with oxygen. These radicals help in the decomposition of ammonia via the H-abstraction reactions shown in R1-R3. Since the concentration of C_3-C_4 species in natural gas is very low (<0.01%), the pathways of decomposition of these species are not significant for the mixture under consideration except for their contribution to the initial radical pool.

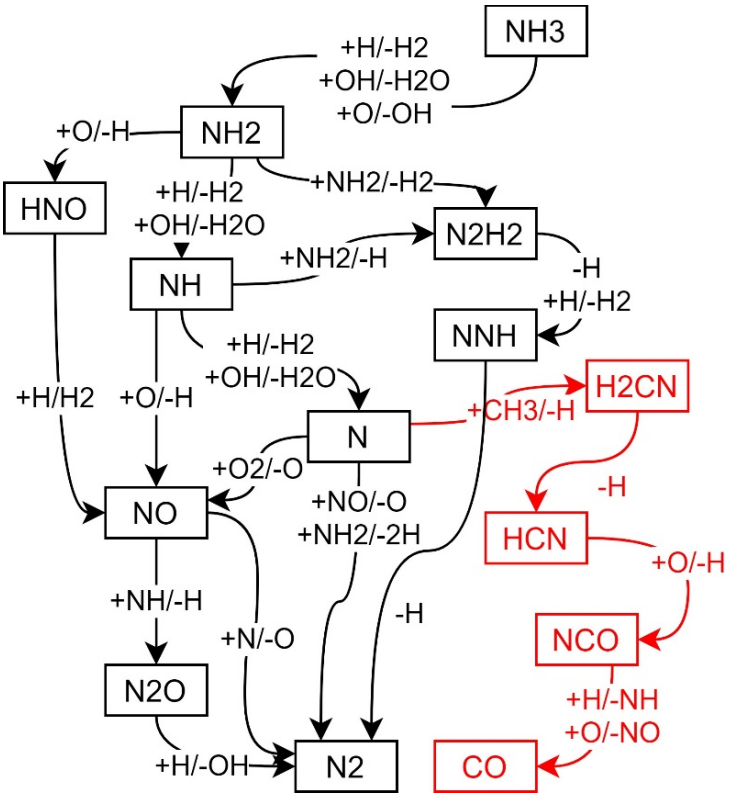

Figure 23: Important Consumption Pathways of NH_3 and its Intermediates during NH_3 Oxidation at 1600 K and 2 atm (Pathway in Red Takes Place only in Presence of Natural Gas)

The NH_2 formed from ammonia decomposition also helps in promoting the decomposition of methane and ethane by H-abstraction reactions R10 and R11. The NH2 formed then undergoes reaction R4-R9 to form HNO, NH, and N_2H_2. The methyl radical formed from natural gas helps in H-abstraction from N_2H_2 to form NNH by reaction R12.

$$CH_4 + NH_2 = CH_3 + NH_3 \quad \text{R10}$$

$$C_2H_6 + NH_2 = C_2H_5 + NH_3 \quad \text{R11}$$

$$N_2H_2 + CH_3 = NNH + CH_4 \quad \text{R12}$$

The nitrogen atoms formed from reaction R13 reacts with the methyl radical to form H_2CN, which undergoes hydrogen elimination to form HCN. The HCN then reacts with O radical to form NCO eventually forming carbon monoxide (R13-R18).

$NH + H = N + H_2$ R13

$CH_3 + N = H_2CN + H$ R14

$H_2CN + M = HCN + H + M$ R15

$HCN + O = NCO + H$ R16

$NCO + H = NH + CO$ R17

$NCO + O = NO + CO$ R18

CHAPTER 5: CONCLUSION

In this work, the authors offered the needed experimental data for natural gas + NH_3 and natural gas + H_2 mixtures to better understand the combustion phenomena at engine-relevant conditions. It was found that hydrogen addition to natural gas decreases the ignition delay times during combustion to a significant degree while ammonia addition was shown to have varying effects depending on the fuel composition. 1% natural gas + 1% ammonia resulted in a large increase in the ignition delay times, while 1% natural gas + 0.1% ammonia showed a slight decrease in ignition delay times, indicating the importance of the ammonia fraction in the mixture and equivalence ratio on the combustion characteristics. For the neat hydrogen comparison, it was found that ammonia addition delayed ignition. IDTs increased at both low temperatures and high temperatures with large variance at both conditions. A chemical kinetic model 'UCF 2022' was compiled and the predictions were found to be in good agreement with experimental results. A sensitivity analysis and a reaction path analysis have been conducted and important reactions involved in ammonia oxidation in the presence of hydrogen and natural gas have been identified.

REFERENCES

[1] Lindstrom, P., 2019, "EIA projects global energy-related CO2 emissions will increase through 2050."

[2] Brown, T., 2018, "Ammonia for Power: a literature review," https://www.ammoniaenergy.org/articles/ammonia-for-power-a-literature-review/.

[3] Bull, D. C., 1968, "A shock tube study of the oxidation of ammonia," Combustion and Flame, 12(6), pp. 603-610.

[4] Takeyama Tetsu, M. H., 1966, "Kinetic Studies of Ammonia Oxidation in Shock Waves. II. The Rate of Ammonia Consumption," Bulletin of the Chemical Society of Japan, 39(11), pp. 2352-2355.

[5] Tetsu Takeyama, H. M., 1965, "Kinetic Studies of Ammonia Oxidation in Shock Waves. I. The Reaction Mechanism for the Induction Period," Bulletin of the Chemical Society of Japan, 38(10), pp. 1670-1674.

[6] Tetsu Takeyama, H. M., 1967, Eleventh Symposium (International) on Combustion, The Combustion Institute: Pittsburgh Pittsburgh.

[7] Soloukhin, R. I., 1967, Eleventh Symposium (International) on Combustion, The Combustion Institute: Pittsburgh Pittsburgh.

[8] L.J. Drummond, S. W. H., 1966, "SHOCK-INITIATED EXOTHERMIC REACTIONS. II. THE OXIDATION OF AMMONIA," Australian Journal of Chemistry, 20, pp. 825-836.

[9] J.N. Bradley, R. N. B., D. Lewis, 1968, "Oxidation of Ammonia in Shock Waves," Royal Society of Chemistry, 64.

[10] He, X., Shu, B., Nascimento, D., Moshammer, K., Costa, M., and Fernandes, R. X., 2019, "Auto-ignition kinetics of ammonia and ammonia/hydrogen mixtures at intermediate

temperatures and high pressures," Combustion and Flame, 206, pp. 189-200.

[11] Song, Y., Hashemi, H., Christensen, J. M., Zou, C., Marshall, P., and Glarborg, P., 2016, "Ammonia oxidation at high pressure and intermediate temperatures," Fuel, 181, pp. 358-365.

[12] Iki, N., Kurata, O., Matsunuma, T., Inoue, T., Tsujimura, T., Furutani, H., Kobayashi, H., and Hayakawa, A., 2017, "Operation and Flame Observation of Micro Gas Turbine Firing Ammonia," ASME Turbo Expo 2017: Turbomachinery Technical Conference and Exposition.

[13] Iki, N., Kurata, O., Matsunuma, T., Inoue, T., Tsujimura, T., Furutani, H., Kobayashi, H., Hayakawa, A., Arakawa, Y., and Ichikawa, A., 2016, "Micro Gas Turbine Firing Ammonia," ASME Turbo Expo 2016: Turbomachinery Technical Conference and Exposition.

[14] Mathieu, O. and Petersen, E. L., 2015, "Experimental and modeling study on the high-temperature oxidation of Ammonia and related NOx chemistry," Combustion and Flame, 162(3), pp. 554-570.

[15] Mei, B., Ma, S., Zhang, Y., Zhang, X., Li, W., and Li, Y., 2020, "Exploration on laminar flame propagation of ammonia and syngas mixtures up to 10 atm," Combustion and Flame, 220, pp. 368-377.

[16] Okafor, E. C., Somarathne, K. D. K. A., Ratthanan, R., Hayakawa, A., Kudo, T., Kurata, O., Iki, N., Tsujimura, T., Furutani, H., and Kobayashi, H., 2020, "Control of NOx and other emissions in micro gas turbine combustors fuelled with mixtures of methane and ammonia," Combustion and Flame, 211, pp. 406-416.

[17] Otomo, J., Koshi, M., Mitsumori, T., Iwasaki, H., and Yamada, K., 2018, "Chemical kinetic

modeling of ammonia oxidation with improved reaction mechanism for ammonia/air and ammonia/hydrogen/air combustion," International Journal of Hydrogen Energy, 43(5), pp. 3004-3014.

[18] Mathieu, O., Kopp, M. M., and Petersen, E. L., 2013, "Shock-tube study of the ignition of multi-component syngas mixtures with and without ammonia impurities," Proceedings of the Combustion Institute, 34(2), pp. 3211-3218.

[19] Shu, B., Vallabhuni, S. K., He, X., Issayev, G., Moshammer, K., Farooq, A., and Fernandes, R. X., 2019, "A shock tube and modeling study on the autoignition properties of ammonia at intermediate temperatures," Proceedings of the Combustion Institute, 37(1), pp. 205-211.

[20] da Rocha, R. C., Costa, M., and Bai, X.-S., 2019, "Chemical kinetic modelling of ammonia/hydrogen/air ignition, premixed flame propagation and NO emission," Fuel, 246, pp. 24-33.

[21] Chen, J., Jiang, X., Qin, X., and Huang, Z., 2021, "Effect of hydrogen blending on the high temperature auto-ignition of ammonia at elevated pressure," Fuel, 287, p. 119563.

[22] Valera-Medina, A., Pugh, D. G., Marsh, P., Bulat, G., and Bowen, P., 2017, "Preliminary study on lean premixed combustion of ammonia-hydrogen for swirling gas turbine combustors," International Journal of Hydrogen Energy, 42(38), pp. 24495-24503.

[23] Pochet, M., Dias, V., Moreau, B., Foucher, F., Jeanmart, H., and Contino, F., 2019, "Experimental and numerical study, under LTC conditions, of ammonia ignition delay with and without hydrogen addition," Proceedings of the Combustion Institute, 37(1), pp. 621-629.

[24] Li, J., Huang, H., Kobayashi, N., Wang, C., and Yuan, H., 2017, "Numerical study on

laminar burning velocity and ignition delay time of ammonia flame with hydrogen addition," Energy, 126, pp. 796-809.

[25] Oh, S., Park, C., Kim, S., Kim, Y., Choi, Y., and Kim, C., 2021, "Natural gas–ammonia dual-fuel combustion in spark-ignited engine with various air–fuel ratios and split ratios of ammonia under part load condition," Fuel, 290, p. 120095.

[26] Ishaq, H., and Dincer, I., 2020, "A comprehensive study on using new hydrogen-natural gas and ammonia-natural gas blends for better performance," Journal of Natural Gas Science and Engineering, 81, p. 103362.

[27] Shintaro Ito*, M. U., Shogo Onishi, Soichiro Kato, Toshiro Fujimori, IHI Corporation, Japan; Hideaki Kobayashi, , 2018, "Performance of Ammonia-Natural Gas Co-Fired Gas Turbine for Power Generation," 15th Annual NH3 Fuel Conference, NH3 Fuel Association, Pittsburgh, PA.

[28] Shogo Onishi, S. I., Masahiro Uchida, Soichiro Kato, Tsukasa Saito, Toshiro Fujimori, Hideaki Kobayashi, "Methods for Low NOx Combustion in Ammonia/Natural Gas Dual Fuel Gas Turbine Combustor," Proc. AIChE Annual Meeting.

[29] Reiter, A. J., and Kong, S.-C., 2008, "Demonstration of Compression-Ignition Engine Combustion Using Ammonia in Reducing Greenhouse Gas Emissions," Energy & Fuels, 22(5), pp. 2963-2971.

[30] Koroglu, B., Neupane, S., Pryor, O., Peale, R. E., and Vasu, S. S., 2018, "High temperature infrared absorption cross sections of methane near 3.4 μm in Ar and CO2 mixtures," Journal of Quantitative Spectroscopy and Radiative Transfer, 206, pp. 36-45.

[31] Koroglu, B., Pryor, O. M., Lopez, J., Nash, L., and Vasu, S. S., 2016, "Shock tube ignition delay times and methane time-histories measurements during excess CO2 diluted oxy-

methane combustion," Combustion and Flame, 164, pp. 152-163.

[32] Pryor, O., Barak, S., Lopez, J., Ninnemann, E., Koroglu, B., Nash, L., and Vasu, S., 2017, "High Pressure Shock Tube Ignition Delay Time Measurements During Oxy-Methane Combustion With High Levels of CO2 Dilution," Journal of Energy Resources Technology, 139(4).

[33] D. F. Davidson, R. K. H., 2004, "Interpreting shock tube ignition data," International Journal of Chemical Kinetics, 36(9), pp. 510-523.

[34] Ninnemann, E., Kim, G., Laich, A., Almansour, B., Terracciano, A. C., Park, S., Thurmond, K., Neupane, S., Wagnon, S., Pitz, W. J., and Vasu, S. S., 2019, "Co-optima fuels combustion: A comprehensive experimental investigation of prenol isomers," Fuel, 254, p. 115630.

[35] Rothman, L. S., Gordon, I. E., Babikov, Y., Barbe, A., Chris Benner, D., Bernath, P. F., Birk, M., Bizzocchi, L., Boudon, V., Brown, L. R., Campargue, A., Chance, K., Cohen, E. A., Coudert, L. H., Devi, V. M., Drouin, B. J., Fayt, A., Flaud, J. M., Gamache, R. R., Harrison, J. J., Hartmann, J. M., Hill, C., Hodges, J. T., Jacquemart, D., Jolly, A., Lamouroux, J., Le Roy, R. J., Li, G., Long, D. A., Lyulin, O. M., Mackie, C. J., Massie, S. T., Mikhailenko, S., Müller, H. S. P., Naumenko, O. V., Nikitin, A. V., Orphal, J., Perevalov, V., Perrin, A., Polovtseva, E. R., Richard, C., Smith, M. A. H., Starikova, E., Sung, K., Tashkun, S., Tennyson, J., Toon, G. C., Tyuterev, V. G., and Wagner, G., 2013, "The HITRAN2012 molecular spectroscopic database," Journal of Quantitative Spectroscopy and Radiative Transfer, 130, pp. 4-50.

[36] 2011, "CHEMKIN-PRO," R. Design, ed.San Diego, CA.

[37] Rahman, R. K., Barak, S., Manikantachari, K. R. V., Ninnemann, E., Hosangadi, A.,

Zambon, A., and Vasu, S. S., 2020, "Probing the Effects of NOx and SOx Impurities on Oxy-Fuel Combustion in Supercritical CO2: Shock Tube Experiments and Chemical Kinetic Modeling," Journal of Energy Resources Technology, 142(12).

[38] Zhou, C.-W., Li, Y., Burke, U., Banyon, C., Somers, K. P., Ding, S., Khan, S., Hargis, J. W., Sikes, T., Mathieu, O., Petersen, E. L., AlAbbad, M., Farooq, A., Pan, Y., Zhang, Y., Huang, Z., Lopez, J., Loparo, Z., Vasu, S. S., and Curran, H. J., 2018, "An experimental and chemical kinetic modeling study of 1,3-butadiene combustion: Ignition delay time and laminar flame speed measurements," Combustion and Flame, 197, pp. 423-438.

[39] Dean, A. M., and Bozzelli, J. W., 2000, "Combustion chemistry of nitrogen," Gas-phase combustion chemistry, Springer, pp. 125-341.